Published in final edited form as:
Cancer Cell. 2013 March 18; 23(3): 287–301. doi:10.1016/j.ccr.2012.11.020.

PGC1α Expression Defines a Subset of Human Melanoma Tumors with Increased Mitochondrial Capacity and Resistance to Oxidative Stress

Francisca Vazquez[1,†], **Ji-Hong Lim**[1,†], **Helen Chim**[1], **Kavita Bhalla**[2], **Geoff Girnun**[2], **Kerry Pierce**[3], **Clary B. Clish**[3], **Scott R. Granter**[4], **Hans R. Widlund**[5], **Bruce M. Spiegelman**[1], and **Pere Puigserver**[1,*]

[1]Department of Cancer Biology, Dana-Farber Cancer Institute and Department of Cell Biology, Harvard Medical School, Boston, MA 02115, USA

[2] Stewart Greenebaum Cancer Center, Department of Pathology, University of Maryland School of Medicine, Baltimore, MD 21201, USA

[3] Metabolite Profiling Initiative, Broad Institute of MIT and Harvard, 7 Cambridge Center, Cambridge, MA 02142

[4] Department of Pathology, Harvard Skin Disease Research Center, Brigham and Women's Hospital, Boston, MA 02115, USA

[5] Department of Dermatology, Harvard Skin Disease Research Center, Brigham and Women's Hospital, Boston, MA 02115, USA

SUMMARY

Cancer cells reprogram their metabolism using different strategies to meet energy and anabolic demands to maintain growth and survival. Understanding the molecular and genetic determinants of these metabolic programs is critical to successfully exploit them for therapy. Here, we report that the oncogenic melanocyte lineage-specification transcription factor MITF drives PGC1α (PPARGC1A) overexpression in a subset of human melanomas and derived cell lines. Functionally, PGC1α positive melanoma cells exhibit increased mitochondrial energy metabolism and ROS detoxification capacities that enables survival under oxidative stress conditions. Conversely, PGC1α negative melanoma cells are more glycolytic and sensitive to ROS-inducing drugs. These results demonstrate that differences in PGC1α levels in melanoma tumors have a profound impact in their metabolism, biology and drug sensitivity.

INTRODUCTION

Tumors reprogram their metabolism to meet increased energetic and anabolic demands. A frequent metabolic adaptation that cancer cells acquire is an increase in glucose uptake and

[*]**Corresponding author:** Dr. Pere Puigserver Dana-Farber Cancer Institute 450 Brookline Av. CLSB-11144 Boston, MA 02215 Phone: 617-582-7977 Fax: 617-632-5363 pere_puigserver@dfci.harvard.edu.
[†]Equal Contribution

Accession Numbers
The Gene Expression Omnibus accession number for the gene expression data reported is GSE36879.

aerobic glycolysis together with decrease in oxidative metabolism. It is clear, however, that there is not one single tumor-specific metabolic state and tumors can utilize a variety of different metabolic strategies that have only now begun to be elucidated. For example, tumor cells are able to generate ATP through mitochondrial oxidation of fatty acids and amino acids such as glutamine when glucose becomes limiting (Zaugg et al., 2011) (Choo et al., 2010) (Gao et al., 2009) (Wise et al., 2008).

An increase in reactive oxygen species (ROS), due to an enhanced and unbalanced metabolic activity (Hanahan and Weinberg, 2011) is a common stressor to which tumors must adapt. This increased generation of ROS can play a dual role in the cancer phenotype. On one hand, it can play a tumorigenic role by stimulating cell proliferation and promoting genomic instability (Weinberg and Chandel, 2009). On the other hand, above a certain threshold, ROS can be toxic and induce cellular damage, leading to cell death (Trachootham et al., 2009) (Diehn et al., 2009). Cancer cells develop adaptive responses against oxidative stress, often by upregulating their antioxidant scavenging capacity. One clear example is the constitutive activation of the Keap1-Nrf2 pathway in squamous cell carcinomas, either by activating mutations in Nrf2 or through inactivating mutations in KEAP1 (an Nrf2 cytoplasmic repressor) (Padmanabhan et al., 2006) (Singh et al., 2006) (Shibata et al., 2008) (Ohta et al., 2008). Whereas some of these components of the oxidative stress response have been identified in cancer cells, it is likely that key regulators in this response that contribute to tumorigenesis are still missing.

PPARGC1A, named hereafter PGC1α, is part of a small family of transcriptional coactivators, including PGC1β and PRC, that promote mitochondrial biogenesis and respiration (Puigserver and Spiegelman, 2003) (Scarpulla, 2011). PGC1α is the best studied, particularly in brown fat, skeletal and cardiac muscle, liver and fat tissues where it is a key regulator of mitochondrial mass, thermogenic programs and adaptation to fasting conditions (Kelly and Scarpulla, 2004). PGC1α can also potently reduce generation of mitochondrial-driven ROS (St-Pierre et al., 2006). PGC1α is typically expressed at low levels under normal conditions and is strongly induced and activated in response to increased metabolic and energetic demands in highly metabolic tissues. For example, exercise increases PGC1α levels in skeletal muscle where it induces mitochondrial biogenesis and oxidative capacity (Handschin et al., 2007). Cold exposure rapidly increases PGC1α levels in brown/beige adipose tissue to program a thermogenic response based on mitochondrial function (Puigserver et al., 1998). In liver, fasting increases PGC1α to induce fatty acid oxidation, hepatic glucose production and ketogenesis (Rhee et al., 2003). In many of these cell types, the cAMP pathway plays a central role through the activation of a CREB response element at the PGC1α promoter (Herzig et al., 2001). Other signals contribute to increases in PGC1α gene expression such as calcium signaling and MEF2 transcriptional activity in skeletal muscle (Lin et al., 2002). It is unknown, however, whether and how oncogenic signals impact PGC1α expression and what are the metabolic and growth consequences this might cause to the tumor phenotype.

RESULTS

A Subset of Human Melanoma Tumors Expresses High Levels of PGC1α and Mitochondrial Genes of Oxidative Metabolism

Given the central role of PGC1α in oxidative metabolism and ROS detoxification in a variety of tissues (Puigserver and Spiegelman, 2003) (Kelly and Scarpulla, 2004) (Fernandez-Marcos and Auwerx, 2011) (St-Pierre et al., 2006), we hypothesized that PGC1α could be aberrantly activated in some tumors and thereby conferring them an adaptive advantage. Since PGC1α is strongly regulated at the mRNA level, publicly available gene expression databases were surveyed. In several data sets, a subset of

melanoma tumors and melanoma derived cell lines expressed very high relative levels of PGC1α mRNA. Figures 1A and S1A show the relative PGC1α mRNA levels from 56 melanoma tumors (GSE7553) (Riker et al., 2008) and 82 short-term melanoma cultures (Lin et al., 2008). 10.7% for Riker melanoma data set and 8.4% for short-term melanoma cultures showed PGC1α expression levels that are at least one standard deviation above the average. To assess if the high PGC1α levels in these melanoma tumors were associated with its known metabolic gene expression program, we used Gene Set Enrichment Analysis (GSEA) to find gene expression signatures that correlated with PGC1α expression. Consistent with previous and established PGC1α targets in skeletal muscle cells (Mootha et al., 2003), gene expression sets of mitochondrial genes, energy metabolism and ESRRA target genes were all significantly correlated with PGC1α expression in both melanoma tumors and short-term melanoma cultures (Table 1 and Table S1). Using an additional data set of metastatic melanoma tumors with clinical outcome data (Bogunovic et al., 2009) we found that tumors expressing high PGC1α levels were associated with lower survival (long-rank p value 0.0230) compared to low PGC1α expressing tumors (Figure 1B). The high and low expressing tumors were defined by selecting the top and bottom 25% PGC1α expressing tumors. Other clinical parameters were not affected (Figure S1B). The overexpression results were validated using patient derived long-term melanoma cell lines. Remarkably, all melanoma cell lines tested fell into two categories with very high levels (PGC1α positive) or undetectable or very low levels (PGC1α negative) of PGC1α mRNA (Figure 1C) and protein (Figure 1D). PGC1α positive cell lines had elevated levels of mitochondrial respiratory chain proteins from all different complexes tested (Figure 1D). These results suggest that PGC1α induces a mitochondrial metabolism gene expression program in these tumors and tumor derived cell lines. To confirm that PGC1α was driving the mitochondrial metabolism gene expression signature, we used lentiviral shRNA to reduce its expression in a PGC1α positive melanoma cell line (A375P) and performed gene-expression microarray followed by GSEA analysis. Similar gene expression sets of mitochondrial energy metabolism, as the ones found in melanoma tumors and short-term melanoma cultures, were enriched in control versus PGC1α knock-down cell lines (Figure 1E, Table S2). Some of the targets were confirmed using qPCR in A375P and two other PGC1α positive melanoma cell lines (MeWo and G361) (Figure 1F). As expected, downregulation of mitochondrial genes in PGC1α depleted A375P cells translated into decreases of protein levels. Several components of the oxidative phosphorylation complex were substantially decreased in PGC1α knock-down cells, particularly proteins that are part of Complex I and Complex IV (Figure 1G). PGC1α expression was also sufficient to induce this mitochondrial program. Modest ectopic expression of PGC1α in a PGC1α negative cell line (A375, a metastatic clone derived from A375P) increased mitochondrial gene targets and protein levels (Figures S1C, S1D). We then next compared the levels of PGC1α between non-transformed melanocytes and melanoma cells. The relative levels of PGC1α mRNA expression were measured in cultured immortal primary melanocytes and in a PGC1α positive and negative cell line. PGC1α mRNA expression levels in primary melanocytes were higher than PGC1α negative cells but dramatically lower than PGC1α positive cells (Figure S1E).

Together, these results indicate that PGC1α is overexpressed in a subset of melanoma tumors and drives a mitochondrial gene expression program. Interestingly, the overexpression of PGC1α and correlation with oxidative metabolism is not only present in melanomas. We found that levels of PGC1α expression in lung adenocarcinoma cell lines also correlate with an oxidative metabolism signature (Figure S1 and Table S3).

MITF Expression in Human Melanoma Cells Drives High Levels of PGC1α Gene Expression

In order to identify the key factors responsible for the high levels of PGC1α expression in melanoma, we used publicly available data on gene expression, copy number and mutations

from the CCLE database (www.broadinstitute.org/ccle) (Barretina et al., 2012). We found no correlation between PGC1α copy number levels and gene expression. Only one melanoma cell line (SK-MEL1) -out of 60 melanoma cell lines with copy number data available at the time (Figure S2A, data from the CCLE database)- was found to have PGC1α amplification; suggesting that amplification is not a common mechanism to increase PGC1α expression levels. Since p53 has been shown to negatively regulate PGC1α levels (Sahin et al., 2011) (Sen et al., 2011) we searched if there was an association between p53 mutation status and PGC1α expression, but no correlation was found in 60 cell lines with expression and mutation status data. Similarly, there was no correlation with BRAF mutations status (Figure S2B). Third, the Riker melanoma data set was classified by their PGC1α expression levels to identify genes that were upregulated in high PGC1α versus low PGC1α expressing tumors (Figure 2A). Intriguingly, among the top classifying genes identified was MITF, a melanocyte-lineage transcription factor and *bona fide* melanoma oncogene (Garraway et al., 2005) (Yokoyama et al., 2011) (Bertolotto et al., 2011). Similar results were obtained comparing high versus low expressing PGC1α melanoma cell lines. Furthermore, the levels of several MITF downstream target genes such as SLC45A2, CDK2, PMEL, TYR, TYRP1, MLANA and DCT were also differentially expressed (Figure 2B, data from the CCLE database). Hence, within both melanoma specimens and melanoma cell lines the expression levels of PGC1α correlated with MITF levels indicating that they may be affecting each other in an epistatic manner. To forward this notion, we analyzed mRNA and protein levels of MITF in 5 PGC1α positive and 5 PGC1α negative cell lines. We found that both the mRNA and protein levels were higher in PGC1α positive cell lines (Figure 2C). Interestingly, one of the outlier cell lines (SK-MEL-28) that expresses high levels of MITF but is PGC1α negative, expresses high levels of PGC1β.

Based on these data, we investigated if MITF was a causal driver for the high levels of PGC1α gene expression. Hence, we used lentiviral shRNA to reduce endogenous MITF levels in 3 PGC1α positive melanoma cell lines (A375P, G361 and SK-MEL5) and found that it strongly down-regulated PGC1α both at the mRNA and protein levels (Figure 2D, 2E). Notably, PGC1α expression levels were suppressed even further than the known MITF target tyrosinase. Moreover, PGC1α protein levels were almost undetectable after MITF knock-down. As expected, MITF knock-down-induced PGC1α downregulation resulted in decrease of PGC1α targets including mitochondrial genes (Figure S2C). These results indicate that MITF is necessary to maintain high levels of PGC1α expression in PGC1α positive melanoma cell lines.

Next, we investigated whether MITF was sufficient to induce PGC1α expression in melanoma cell lines. Hence, ectopic expression of MITF using retroviral transduction in A375, a PGC1α negative cell line, caused induction of PGC1α mRNA levels, including PGC1α targets, comparable to the known MITF target genes, TYR and DCT (Figure 2F). Because MITF is a transcription factor it could directly bind the upstream regulatory promoter of PGC1α as this region contains several E-boxes sequences (Figure S2D). Transfection of HEK293T cells with MITF induced a 2Kb PGC1α promoter driving luciferase that was dependent on both E-boxes (Figure 2Ga). Conversely, MITF knock-down experiments in A375P cells reduced the activity of this promoter (Figure 2Gb). In addition, ChiP assays showed that endogenous MITF is bound to the PGC1α promoter (Figure 2H), consistent with previously reported Chip-Seq data set (Strub et al., 2011) (Figure S2E).

Gene expression profiling analysis of melanoma tumors has previously identified two expression signatures associated with proliferative or invasive phenotype. MITF expression was higher in melanoma samples with the proliferative signature and lower in samples with an invasive signature (Hoek et al., 2008). Consistently, we found that melanoma tumors with

high PGC1α levels also correlated with the proliferative signature (Figure S2F). Collectively, these results indicate that MITF is necessary and contributes to the high levels of PGC1α expression found in a subset of human melanoma cells.

PGC1α Defines the Metabolic State of Melanoma Cells

To test whether PGC1α expression levels drive the metabolic program of melanoma cells, we compared key cellular metabolic and bioenergetic parameters between PGC1α positive and negative melanoma cells. PGC1α positive cells exhibited substantial increased basal and maximal oxygen consumption rates (Figure 3A). Additionally, the respiration reserve capacity, calculated by subtracting the basal to the maximal respiration capacity was significantly higher in PGC1α expressing melanoma cells. Glucose uptake was slightly decreased in PGC1α positive cells that paralleled diminished levels of secreted lactate compared to PGC1α negative cells (Figure 3B). Consistent with glycolytic metabolism generating lower ATP levels compared to oxidative metabolism, intracellular ATP levels of PGC1α negative melanoma cell lines were reduced (Figure 3B). These differences in metabolic parameters were caused by PGC1α expression. Depletion of PGC1α levels in A375P largely recapitulated the metabolic and bioenergetic patterns of PGC1α negative cells, e.g. decreased in basal, maximal and reserved oxygen OCR and intracellular ATP levels, decreased glucose uptake and increased lactate production (Figures 3C, 3D). Metabolomic analysis showed that shRNA PGC1α cells had increased glycolytic, but decreased TCA intermediates (Figure S3). In addition, a modest increase in PGC1α levels through forced expression (Figure S1C) in a PGC1α negative cell line resulted in a reversal of these metabolic parameters (Figure 3E). In summary, these results indicate that cells with undetectable levels of PGC1α have lower rates of mitochondrial oxidative metabolism but elevated rates of glycolysis and lactate production consistent with a more pronounced glycolytic “Warburg” state. In contrast, PGC1α positive cells have the reversed metabolic phenotype leading to an elevated cellular energetic state.

PGC1α Positive Melanoma Cells are Dependent on PGC1α for Survival and Tumor Progression

Given the central role of PGC1α in the metabolic and energetic state of a subset of melanoma cells with high expression levels, we investigated whether these cells may have become dependent on PGC1α for survival. Thus, we suppressed the expression of PGC1α in five positive cell lines and measured its effect on cell viability. Figure 4A shows that knock-down of PGC1α significantly decreased cell number. As expected, knock-down of PGC1α had no significant effect on PGC1α negative cells. As an additional control, we tested the effect of RPS6 knock-down in a PGC1α positive and negative cell line and observed a similar effect of decreased cell number in both PGC1α positive and negative cell lines (Figure S4A). Overexpression of PGC1α, similar to MITF, was not sufficient to induce proliferation in PGC1α negative melanoma cells (Figures S4B, S4C and S4D) underscoring the context dependency of the effects. We next investigated the mechanism responsible for the reduced cell number after PGC1α knock-down. PGC1α knock-down resulted in a more than 3 fold induction in the percentage of apoptotic cells in two PGC1α positive cell lines (A375P and MeWo) but not in a negative cell line (A375) (Figure 4B). This apoptosis was mediated through the intrinsic pathway as caspases 9 and 3, but not 8 were activated in PGC1α depleted cells. Other apoptotic markers including cleavage of PARP was also induced in PGC1α knock-down cells (Figure 4C). The apoptotic effect was largely reversed by overexpression of PGC1α, indicating that it is a result of PGC1α depletion (Figure 4D). To further support the involvement of caspases, the inhibitor QVD-OPH significantly reduced the number of cells entering apoptosis (Figure 4E). These results indicate that suppression of PGC1α activates the intrinsic mitochondrial apoptotic pathway and strongly

suggest that PGC1α positive melanoma cells have become dependent on PGC1α for survival.

PGC1α Suppression Results in a Reduction of ROS Detoxification Genes and Increase in ROS Levels Leading to Apoptosis

The fact that the intrinsic apoptotic pathway was activated in PGC1α depleted cells suggested that the mitochondria was involved in the induction of apoptosis. One of the mechanisms by which mitochondrial failure causes apoptosis is through the loss of membrane potential and generation of ROS (Tait and Green, 2010). Consistent with induction of this process, knock-down of PGC1α in A375P cells showed a strong decrease in mitochondrial membrane potential as measured using J-aggregation fluorescent assay (Figure 5A). Intracellular concentrations of ROS were significantly increased in PGC1α depleted cells (Figure 5B) and this was associated with a decrease in GSH, cystathionine and 5-adenosylhomocysteine levels (Figure 5C). Importantly, elevated ROS levels were necessary to mediate apoptosis in PGC1α knock down cells because two different antioxidants, N-acetyl-L-cysteine (NAC) and Trolox, largely suppressed caspase and PARP cleavages and the number of apoptotic cells (Figure 5D). To determine whether ROS detoxification genes decrease in PGC1α depleted cells and might contribute to apoptosis, we analyze the microarray data described in Figure 1. Consistent with previous data in non-tumor cells (St-Pierre et al., 2006), a set of genes involved in the ROS detoxification including different glutathione synthase enzymes, thioredoxins, glutaredoxin, peroxiredoxins and SOD2 were decreased in PGC1α knock down cells. These results were confirmed using qPCR of several of these genes (Figure 5E). SOD2 protein levels were substantially decreased in PGC1α depleted melanoma cells (Figure 5F). Moreover, ectopic expression of PGC1α in A375 increased ROS detoxification genes (Figure 5G). This data supports a key role for PGC1α in activating the ROS detoxification gene program to maintain melanoma cell survival. As we have showed that PGC1α is a target of MITF, we next investigated the role of PGC1α downstream of MITF in promoting survival and proliferation. Overexpression of PGC1α could partially overcome the effects of knock-down MITF on DNA-damage and increase of p27 levels (Figure S5A). In addition, treatment of MITF depleted cells with the antioxidant NAC partially blocked the apoptotic effects (Figure S5B). Together, these results suggest that downregulation of PGC1α contributes to the phenotypic effects of MITF knock-down in PGC1α expressing cells.

Depletion of Several PGC1α Respiratory Chain Targets Mimic the Metabolic and ROS-dependent Apoptotic Effects of PGC1α Suppression

The reduction in ROS detoxification genes and GSH levels could be one of the mechanisms by which depletion of PGC1α in melanoma cells induces intracellular ROS levels. However, defects in mitochondrial bioenergetic function are also known to generate toxic ROS levels. Thus, to understand how PGC1α deficiency caused ROS-mediated apoptosis we tested whether knock-down of different proteins of the mitochondrial respiratory complexes, which are PGC1α targets, produced similar metabolic and apoptotic defects as PGC1α depletion. Therefore, Ndufs3, Cox5a and ATP5b were efficiently knocked-down in A375P melanoma cells (Figure 6A). Individual depletion of these three mitochondrial proteins caused a similar metabolic phenotype as PGC1α knock-down cells, leading to decreases in oxygen consumption and increases in glucose uptake and lactate secretion (Figure 6B, 6C). Consistent with an increase in intracellular ROS levels in these cells, GSH levels were also decreased (Figure 6D). Moreover, increased ROS concentrations caused by depletion of these mitochondrial proteins lead to increased cleavage of pro-apoptotic proteins (Figure 6E, 6F). To support the role of ROS mediating cell death, treatment with antioxidants NAC and Trolox largely prevented PARP cleavage (Figure 6G). Together, these results suggest that PGC1α positive melanoma cells are highly sensitive to the

induction of ROS due, at least in part, to the disruption of the mitochondria respiratory complex.

PGC1α Protects Against ROS Induced Apoptosis in Human Melanoma Cells and Tumors

The increased ROS levels in cancer cells makes them more dependent in their antioxidant capacity for cell survival, a principle that is exploited by anti-cancer drugs such as piperlongumine or PEITC. In fact, transformed cells have been shown to be exquisitely more sensitive to ROS inducing drugs than non-transformed cells (Trachootham et al., 2006) (Raj et al., 2011). Based on the results presented above that PGC1α controls the antioxidant capacity affecting cell survival, we investigated if PGC1α, by reducing ROS levels and enhancing the antioxidant capacity, could influence the sensitivity to ROS-inducing drugs in melanoma cells. Depletion of PGC1α in A375P cells enhanced their sensitivity to apoptosis induced by H_2O_2, PEITC or piperlongumine, all of which are known to increase intracellular ROS concentrations (Trachootham et al., 2006) (Raj et al., 2011). These effects were not generalized to all drugs as the B-Raf inhibitor PLX4032 had similar effects in PGC1α control or knock-down A375P cells (Figure 7A, S6A). Furthermore, similar effects on the sensitivity to these compounds were observed after knock-down of several mitochondrial proteins (Ndufs3, Cox5a and ATP5b) (Figure 7A). Consistent with these results piperlongumine had a more potent effect inducing apoptosis in PGC1α negative cells (Figure 7B, 7C). Furthermore, ROS levels after piperlongumine treatment were higher in the four out of the five PGC1α negative compared to five PGC1α positive cell lines tested (Figure 7D and Figure S6B). To further support the role of PGC1α mediating resistance to ROS-induced apoptosis, ectopic expression of PGC1α in PGC1α negative cell lines prevented piperlongumine-induced cleavage of caspase 9 and PARP (Figure 7E).

Finally, to evaluate the impact of PGC1α depletion on tumor growth, subcutaneous injections of control and PGC1α depleted A375P cells were performed in nude mice and the size of the resulting tumors was measured. As shown in Figure 8A there was a significant reduction in tumor size in PGC1α depleted cells, suggesting that PGC1α is important for tumor progression. Importantly, piperlongumine treatment for 7 days had a greater reduction of tumor volume of xenografts derived from PGC1α knock-down cells compared to control xenografts. The magnitude of these effects correlated with induction of apoptotic markers in these tumors (Figure 8B). The growth of these tumors did not affect body weight (Figure 8C). Collectively, this data suggests that PGC1α expression confers resistance to drugs that induce intracellular ROS levels in melanoma cells and tumors.

DISCUSSION

Cancer cells reprogram their metabolism to meet anabolic and energetic demands necessary for growth and survival. It is becoming clear, however, that tumor cells do not employ a single strategy to accomplish this as cancers can choose from a variety of metabolic programs to meet their demands. Here, we provide a clear example of this metabolic reprogramming heterogeneity by showing that cells derived from the one tumor type can have profound differences in their metabolic state. In melanomas, expression levels of PGC1α metabolically define two types of tumors with different bioenergetic and ROS detoxification capacities, thereby affecting the ability to survive under oxidative stress. It is conceivable that in certain low nutrient conditions elevated mitochondrial capacity might be more efficient to generate ATP necessary for survival without compromising anaplerotic reactions to support cell growth.

Our findings show that a subset of melanoma cells acquires high levels of PGC1α that depend on an increased activity of the melanoma oncogene MITF. This would confer a selective advantage to melanocytic tumor cells by providing a strong protection against

oxidative damage. A large subset of melanoma tumors has very low or undetectable levels of PGC1α that to a large extent overlaps with low levels of MITF. These less differentiated tumors use a different metabolic strategy of increased glycolysis for growth and survival. It is also possible that melanoma tumors transit through different states during tumor progression with high or low expression levels of PGC1α. In fact, we provide here an example of this possibility, the PGC1α negative melanoma cell line A375 was derived from a metastatic tumor produced by the PGC1α positive parental cell line A375P (Clark et al., 2000). It is likely that A375 cells lost their melanocytic differentiation state since they express very low levels of MITF and differentiation markers. Concomitant to this loss of differentiation, they became MITF and PGC1α independent for tumor progression. Thus, similar to MITF, PGC1α effects on melanomagenesis may be context dependent. PGC1α controls MITF gene expression contributing to the maintenance of survival in melanomas. Interestingly, PPARγ, a transcription factor known to bind PGC1α (Puigserver et al., 1998), regulates MITF (Grabacka et al., 2008), suggesting that it might be involved in this process.

These results provide the basis for some potential anti-cancer therapeutic strategies targeting cellular metabolism. PGC1α positive cells depend on PGC1α for survival, suggesting that PGC1α itself or one of its target genes could be a therapeutic target. In this regard, although small molecules targeting PGC1α do not currently exist, inhibitors of ERRs, key PGC1 transcription factor partners (Mootha et al., 2004) (Chang et al., 2011) (Schreiber et al., 2004) (Eichner and Giguere, 2011) (Wende et al., 2005), could potentially be used to inhibit of PGC1α function. Because several transcription factors including NRFs, ERRs and YY1 (Scarpulla, 2011) (Knutti and Kralli, 2001) (Cunningham et al., 2007) control PGC1α function, future studies will focus to assess which transcription factor(s) partners with PGC1α to control mitochondrial function and ROS detoxification genes in melanomas. Our data also shows that PGC1α positive cells are more sensitive to disruption of mitochondrial respiration suggesting that specific inhibition of respiratory chain complexes could be another vulnerability that could be exploited in this tumor subtype. Importantly, melanoma cells can adapt their metabolism and become PGC1α independent, underscoring metabolic flexibility as a potential hurdle on developing drugs against metabolic targets. Conversely, PGC1α negative melanoma cells have reduced bioenergetic capacity together with lower levels of anti-oxidant enzymes. As a result, these tumor cells are more sensitive and vulnerable to toxic oxidative stress. This metabolic vulnerability provides a therapeutic strategy to treat this subtype of melanoma tumors (Figure 7). In fact, here we find that ROS inducing drugs, such as piperlongumine or PEITC, that have been shown to preferentially kill transformed over normal cells (Raj et al., 2011) (Trachootham et al., 2006), showed an enhanced cell death efficacy in PGC1α negative melanoma cells.

In summary, our work has revealed that melanoma tumors present heterogeneous metabolic and energetic states defined by levels of PGC1α expression. These studies illustrate how reprogramming metabolism and energy in tumor cells is genetic and context dependent and how this information might be used to develop cancer therapy targeting regulatory metabolic networks.

EXPERIMENTAL PROCEDURES

Cell Culture and Virus Infection

Melanoma cell lines were cultured in high glucose Dulbecco's modified Eagle's medium supplemented with 10% fetal bovine serum. Immortalized primary melanocytes transduced with pBABE-hygro-hTERT, pLNCX2-CDK4(R24C) and pBABE-puro-p53DD were generated as described (Garraway et al., 2005). Lentiviruses were produced by transfecting HEK293T cells with pLKO and packaging vectors as previously described (Moffat et al., 2006) using polyfect (Qiagen). Retroviral particles were produced by transfecting HEK293T

cells with the pBabe or pWZL vectors and packaging vector (pCL-Ampho) using polyfect (Qiagen). GFP control and Flag-HA-PGC1α adenovirus have been previously described (Lerin et al., 2006).

Animal Studies

All animal studies were performed with an approved protocol from the Beth Israel Deaconess Medical Center Institutional Animal Care and Use Committee (Protocol number 105-2011). For xenograft studies, 1×10^6 A375P cells stably expressing scrambled shRNA control or PGC1α shRNA were injected subcutaneously into the flank of Nude mice (Taconic) in 100 μL of media. After cell injection, mice were incubated for 15 days to allow tumor growth, and then mice were treated with DMSO or piperlongumine (1.5 mg/kg, ip) once a day for 6 days. Tumor volumes were measured with a caliper and calculated using the equation volume = $ab^2/2$, where "a" is the maximal width and "b" is maximal orthogonal width.

Arrays and Gene Set Enrichment Analysis

To generate gene-expression arrays, A375P cells were infected with a control shRNA (shGFP or shScr) or a PGC1α shRNA (described in supplemental methods) in duplicate and selected with puromycin for 48 h. Four days after selection, RNA was extracted and gene-expression arrays were performed using Human Genome U133A 2.0 arrays. To create a gene expression file CEL files were used as input for the GenePattern (www.genepattern.broadinstitute.org) module Expression File Creator using RMA and quantile normalization. The gct file created was used as input for the GSEA analysis.

For the melanoma tumors gene expression analysis, the normalized data set GSE7553 was imported from GEO using the software Gene-e (www.broadinstitute.org/software/gene-e). The melanoma samples from the data set were selected to create a gct file. This gct file was used as input for the GSEA algorithm.

To find differentially expressed genes, the probes values were collapsed using maximum average probe and log2 transformed. The signal to noise marker selection tool from Gene-e was used to find genes differentially expressed between the top and the bottom 25% PGC1α expressing melanoma tumors with 10,000 permutations. The cut-off to select the gene list was fold change >2, FDR q<0.25. For the melanoma cell lines gene expression analysis, the gene-centric RMA normalized CCLE expression data set was used (www.broadinstitute.org/ccle).

The GSEA software v2.0 (http://www.broadinstitute.org/gsea) (Subramanian et al., 2005) was used to perform the GSEA analysis. In all the analysis, the Reactome gene sets were used and the number of permutations was changed to 5000. For the GSEA7553 slice data set, the values of the 219195_at probe (corresponding to PPARGC1A) were used as phenotype and the default parameters were used with the exception that Pearson correlation was computed to rank the genes. For the analysis of the A375P data set, the default parameters were used but the permutation type was changed to gene set.

Oxygen Consumption

The oxygen consumption rate was measured using an optical fluorescent oxygen sensor in a Seahorse Bioscience XF24 Extracellular Flux Analyzer. Briefly, cells were seeded in quadruplicate at equal densities (25,000 cells per well) into XF24 tissue culture plates. Cell media was changed 12 hours after cell seeding into unbuffered DMEM medium [8.3g/L DMEM (Sigma), 200 mM GlutaMax-1 (Invitrogen), 25 mM D-glucose (Sigma), 63.3 mM NaCl (Sigma), and phenol red (Sigma), adjusted pH to 7.4 with NaOH] according to

manufacture's protocol. Oxygen consumption was measured under basal conditions and mitochondrial uncoupler FCCP (2 μM). Oxygen consumption values were normalized to cell number.

Intracellular ROS and Cellular GSH Levels

To measure intracellular ROS levels, 2 μM DCF-DA (Invitrogen) was used as a fluorescent dye. Equal number of cells were seeded in 6 well plates, after 72 h cells were trypsinized, washed once with PBS and stained with DCF-DA in Hank's balanced salt solution for 30 min at 37°C. Samples were then immediately analyzed by flow cytometry.

A glutathione colorimetric detection kit (BioVision Research Products) was used to measure total cellular glutathione according to manufacturer's instructions.

Supplementary Material

Refer to Web version on PubMed Central for supplementary material.

Acknowledgments

We thank the Dana-Farber Cancer Institute Microarray Core Facility for performing the gene-expression arrays and the Dana-Farber RNAi facility for the shRNA constructs. These studies were funded by the Claudia Adams Barr Program in Cancer Research and Dana-Farber Cancer Institute funds. HRW acknowledges support from P50CA093683.

REFERENCES

Barretina J, Caponigro G, Stransky N, Venkatesan K, Margolin AA, Kim S, Wilson CJ, Lehar J, Kryukov GV, Sonkin D, et al. The Cancer Cell Line Encyclopedia enables predictive modelling of anticancer drug sensitivity. Nature. 2012; 483:603–607. [PubMed: 22460905]

Bertolotto C, Lesueur F, Giuliano S, Strub T, de Lichy M, Bille K, Dessen P, d'Hayer B, Mohamdi H, Remenieras A, et al. A SUMOylation-defective MITF germline mutation predisposes to melanoma and renal carcinoma. Nature. 2011; 480:94–98. [PubMed: 22012259]

Bogunovic D, O'Neill DW, Belitskaya-Levy I, Vacic V, Yu YL, Adams S, Darvishian F, Berman R, Shapiro R, Pavlick AC, et al. Immune profile and mitotic index of metastatic melanoma lesions enhance clinical staging in predicting patient survival. Proceedings of the National Academy of Sciences of the United States of America. 2009; 106:20429–20434. [PubMed: 19915147]

Chang CY, Kazmin D, Jasper JS, Kunder R, Zuercher WJ, McDonnell DP. The Metabolic Regulator ERRalpha, a Downstream Target of HER2/IGF-1R, as a Therapeutic Target in Breast Cancer. Cancer cell. 2011; 20:500–510. [PubMed: 22014575]

Choo AY, Kim SG, Vander Heiden MG, Mahoney SJ, Vu H, Yoon SO, Cantley LC, Blenis J. Glucose addiction of TSC null cells is caused by failed mTORC1-dependent balancing of metabolic demand with supply. Molecular cell. 2010; 38:487–499. [PubMed: 20513425]

Clark EA, Golub TR, Lander ES, Hynes RO. Genomic analysis of metastasis reveals an essential role for RhoC. Nature. 2000; 406:532–535. [PubMed: 10952316]

Cunningham JT, Rodgers JT, Arlow DH, Vazquez F, Mootha VK, Puigserver P. mTOR controls mitochondrial oxidative function through a YY1-PGC-1alpha transcriptional complex. Nature. 2007; 450:736–740. [PubMed: 18046414]

Diehn M, Cho RW, Lobo NA, Kalisky T, Dorie MJ, Kulp AN, Qian D, Lam JS, Ailles LE, Wong M, et al. Association of reactive oxygen species levels and radioresistance in cancer stem cells. Nature. 2009; 458:780–783. [PubMed: 19194462]

Eichner LJ, Giguere V. Estrogen related receptors (ERRs): a new dawn in transcriptional control of mitochondrial gene networks. Mitochondrion. 2011; 11:544–552. [PubMed: 21497207]

Fernandez-Marcos PJ, Auwerx J. Regulation of PGC-1alpha, a nodal regulator of mitochondrial biogenesis. The American journal of clinical nutrition. 2011; 93:884S–890. [PubMed: 21289221]

Gao P, Tchernyshyov I, Chang TC, Lee YS, Kita K, Ochi T, Zeller KI, De Marzo AM, Van Eyk JE, Mendell JT, Dang CV. c-Myc suppression of miR-23a/b enhances mitochondrial glutaminase expression and glutamine metabolism. Nature. 2009; 458:762–765. [PubMed: 19219026]

Garraway LA, Widlund HR, Rubin MA, Getz G, Berger AJ, Ramaswamy S, Beroukhim R, Milner DA, Granter SR, Du J, et al. Integrative genomic analyses identify MITF as a lineage survival oncogene amplified in malignant melanoma. Nature. 2005; 436:117–122. [PubMed: 16001072]

Grabacka M, Placha W, Urbanska K, Laidler P, Plonka PM, Reiss K. PPAR gamma regulates MITF and beta-catenin expression and promotes a differentiated phenotype in mouse melanoma S91. Pigment cell & melanoma research. 2008; 21:388–396. [PubMed: 18444964]

Hanahan D, Weinberg RA. Hallmarks of cancer: the next generation. Cell. 2011; 144:646–674. [PubMed: 21376230]

Handschin C, Chin S, Li P, Liu F, Maratos-Flier E, Lebrasseur NK, Yan Z, Spiegelman BM. Skeletal muscle fiber-type switching, exercise intolerance, and myopathy in PGC-1alpha muscle-specific knock-out animals. The Journal of biological chemistry. 2007; 282:30014–30021. [PubMed: 17702743]

Herzig S, Long F, Jhala US, Hedrick S, Quinn R, Bauer A, Rudolph D, Schutz G, Yoon C, Puigserver P, et al. CREB regulates hepatic gluconeogenesis through the coactivator PGC-1. Nature. 2001; 413:179–183. [PubMed: 11557984]

Hoek KS, Eichhoff OM, Schlegel NC, Dobbeling U, Kobert N, Schaerer L, Hemmi S, Dummer R. In vivo switching of human melanoma cells between proliferative and invasive states. Cancer research. 2008; 68:650–656. [PubMed: 18245463]

Kelly DP, Scarpulla RC. Transcriptional regulatory circuits controlling mitochondrial biogenesis and function. Genes & development. 2004; 18:357–368. [PubMed: 15004004]

Knutti D, Kralli A. PGC-1, a versatile coactivator. Trends in endocrinology and metabolism: TEM. 2001; 12:360–365. [PubMed: 11551810]

Lerin C, Rodgers JT, Kalume DE, Kim SH, Pandey A, Puigserver P. GCN5 acetyltransferase complex controls glucose metabolism through transcriptional repression of PGC-1alpha. Cell metabolism. 2006; 3:429–438. [PubMed: 16753578]

Lin J, Wu H, Tarr PT, Zhang CY, Wu Z, Boss O, Michael LF, Puigserver P, Isotani E, Olson EN, et al. Transcriptional co-activator PGC-1 alpha drives the formation of slow-twitch muscle fibres. Nature. 2002; 418:797–801. [PubMed: 12181572]

Lin WM, Baker AC, Beroukhim R, Winckler W, Feng W, Marmion JM, Laine E, Greulich H, Tseng H, Gates C, et al. Modeling genomic diversity and tumor dependency in malignant melanoma. Cancer research. 2008; 68:664–673. [PubMed: 18245465]

Moffat J, Grueneberg DA, Yang X, Kim SY, Kloepfer AM, Hinkle G, Piqani B, Eisenhaure TM, Luo B, Grenier JK, et al. A lentiviral RNAi library for human and mouse genes applied to an arrayed viral high-content screen. Cell. 2006; 124:1283–1298. [PubMed: 16564017]

Mootha VK, Handschin C, Arlow D, Xie X, St Pierre J, Sihag S, Yang W, Altshuler D, Puigserver P, Patterson N, et al. Err{alpha} and Gabpa/b specify PGC-1{alpha}-dependent oxidative phosphorylation gene expression that is altered in diabetic muscle. Proceedings of the National Academy of Sciences of the United States of America. 2004; 101:6570–6575. [PubMed: 15100410]

Mootha VK, Lindgren CM, Eriksson KF, Subramanian A, Sihag S, Lehar J, Puigserver P, Carlsson E, Ridderstrale M, Laurila E, et al. PGC-1 alpha-responsive genes involved in oxidative phosphorylation are coordinately downregulated in human diabetes. Nat Genet. 2003; 34:267–273. [PubMed: 12808457]

Ohta T, Iijima K, Miyamoto M, Nakahara I, Tanaka H, Ohtsuji M, Suzuki T, Kobayashi A, Yokota J, Sakiyama T, et al. Loss of Keap1 function activates Nrf2 and provides advantages for lung cancer cell growth. Cancer research. 2008; 68:1303–1309. [PubMed: 18316592]

Padmanabhan B, Tong KI, Ohta T, Nakamura Y, Scharlock M, Ohtsuji M, Kang MI, Kobayashi A, Yokoyama S, Yamamoto M. Structural basis for defects of Keap1 activity provoked by its point mutations in lung cancer. Molecular cell. 2006; 21:689–700. [PubMed: 16507366]

Puigserver P, Spiegelman BM. Peroxisome proliferator-activated receptor-gamma coactivator 1 alpha (PGC-1 alpha): transcriptional coactivator and metabolic regulator. Endocrine reviews. 2003; 24:78–90. [PubMed: 12588810]

Puigserver P, Wu Z, Park CW, Graves R, Wright M, Spiegelman BM. A cold-inducible coactivator of nuclear receptors linked to adaptive thermogenesis. Cell. 1998; 92:829–839. [PubMed: 9529258]

Raj L, Ide T, Gurkar AU, Foley M, Schenone M, Li X, Tolliday NJ, Golub TR, Carr SA, Shamji AF, et al. Selective killing of cancer cells by a small molecule targeting the stress response to ROS. Nature. 2011; 475:231–234. [PubMed: 21753854]

Rhee J, Inoue Y, Yoon JC, Puigserver P, Fan M, Gonzalez FJ, Spiegelman BM. Regulation of hepatic fasting response by PPARgamma coactivator-1alpha (PGC-1): requirement for hepatocyte nuclear factor 4alpha in gluconeogenesis. Proceedings of the National Academy of Sciences of the United States of America. 2003; 100:4012–4017. [PubMed: 12651943]

Riker AI, Enkemann SA, Fodstad O, Liu S, Ren S, Morris C, Xi Y, Howell P, Metge B, Samant RS, et al. The gene expression profiles of primary and metastatic melanoma yields a transition point of tumor progression and metastasis. BMC medical genomics. 2008; 1:13. [PubMed: 18442402]

Sahin E, Colla S, Liesa M, Moslehi J, Muller FL, Guo M, Cooper M, Kotton D, Fabian AJ, Walkey C, et al. Telomere dysfunction induces metabolic and mitochondrial compromise. Nature. 2011; 470:359–365. [PubMed: 21307849]

Scarpulla RC. Metabolic control of mitochondrial biogenesis through the PGC-1 family regulatory network. Biochimica et biophysica acta. 2011; 1813:1269–1278. [PubMed: 20933024]

Schreiber SN, Emter R, Hock MB, Knutti D, Cardenas J, Podvinec M, Oakeley EJ, Kralli A. The estrogen-related receptor {alpha} (ERR{alpha}) functions in PPAR{gamma} coactivator 1{alpha} (PGC-1{alpha})-induced mitochondrial biogenesis. Proceedings of the National Academy of Sciences of the United States of America. 2004; 101:6472–6477. [PubMed: 15087503]

Sen N, Satija YK, Das S. PGC-1alpha, a key modulator of p53, promotes cell survival upon metabolic stress. Molecular cell. 2011; 44:621–634. [PubMed: 22099309]

Shibata T, Ohta T, Tong KI, Kokubu A, Odogawa R, Tsuta K, Asamura H, Yamamoto M, Hirohashi S. Cancer related mutations in NRF2 impair its recognition by Keap1-Cul3 E3 ligase and promote malignancy. Proceedings of the National Academy of Sciences of the United States of America. 2008; 105:13568–13573. [PubMed: 18757741]

Singh A, Misra V, Thimmulappa RK, Lee H, Ames S, Hoque MO, Herman JG, Baylin SB, Sidransky D, Gabrielson E, et al. Dysfunctional KEAP1-NRF2 interaction in non-small-cell lung cancer. PLoS medicine. 2006; 3:e420. [PubMed: 17020408]

St-Pierre J, Drori S, Uldry M, Silvaggi JM, Rhee J, Jager S, Handschin C, Zheng K, Lin J, Yang W, et al. Suppression of reactive oxygen species and neurodegeneration by the PGC-1 transcriptional coactivators. Cell. 2006; 127:397–408. [PubMed: 17055439]

Strub T, Giuliano S, Ye T, Bonet C, Keime C, Kobi D, Le Gras S, Cormont M, Ballotti R, Bertolotto C, Davidson I. Essential role of microphthalmia transcription factor for DNA replication, mitosis and genomic stability in melanoma. Oncogene. 2011; 30:2319–2332. [PubMed: 21258399]

Subramanian A, Tamayo P, Mootha VK, Mukherjee S, Ebert BL, Gillette MA, Paulovich A, Pomeroy SL, Golub TR, Lander ES, Mesirov JP. Gene set enrichment analysis: a knowledge-based approach for interpreting genome-wide expression profiles. Proceedings of the National Academy of Sciences of the United States of America. 2005; 102:15545–15550. [PubMed: 16199517]

Tait SW, Green DR. Mitochondria and cell death: outer membrane permeabilization and beyond. Nature reviews. 2010; 11:621–632.

Trachootham D, Alexandre J, Huang P. Targeting cancer cells by ROS-mediated mechanisms: a radical therapeutic approach? Nature reviews Drug discovery. 2009; 8:579–591.

Trachootham D, Zhou Y, Zhang H, Demizu Y, Chen Z, Pelicano H, Chiao PJ, Achanta G, Arlinghaus RB, Liu J, Huang P. Selective killing of oncogenically transformed cells through a ROS-mediated mechanism by beta-phenylethyl isothiocyanate. Cancer cell. 2006; 10:241–252. [PubMed: 16959615]

Weinberg F, Chandel NS. Mitochondrial metabolism and cancer. Annals of the New York Academy of Sciences. 2009; 1177:66–73. [PubMed: 19845608]

Wende AR, Huss JM, Schaeffer PJ, Giguere V, Kelly DP. PGC-1alpha coactivates PDK4 gene expression via the orphan nuclear receptor ERRalpha: a mechanism for transcriptional control of muscle glucose metabolism. Molecular and cellular biology. 2005; 25:10684–10694. [PubMed: 16314495]

Wise DR, DeBerardinis RJ, Mancuso A, Sayed N, Zhang XY, Pfeiffer HK, Nissim I, Daikhin E, Yudkoff M, McMahon SB, Thompson CB. Myc regulates a transcriptional program that stimulates mitochondrial glutaminolysis and leads to glutamine addiction. Proceedings of the National Academy of Sciences of the United States of America. 2008; 105:18782–18787. [PubMed: 19033189]

Yokoyama S, Woods SL, Boyle GM, Aoude LG, MacGregor S, Zismann V, Gartside M, Cust AE, Haq R, Harland M, et al. A novel recurrent mutation in MITF predisposes to familial and sporadic melanoma. Nature. 2011; 480:99–103. [PubMed: 22080950]

Zaugg K, Yao Y, Reilly PT, Kannan K, Kiarash R, Mason J, Huang P, Sawyer SK, Fuerth B, Faubert B, et al. Carnitine palmitoyltransferase 1C promotes cell survival and tumor growth under conditions of metabolic stress. Genes & development. 2011; 25:1041–1051. [PubMed: 21576264]

- PGC1α is elevated in a subset of human melanoma tumors and derived cell lines
- PGC1α Positive Melanoma cells exhibit increased mitochondrial metabolism
- PGC1α Positive Melanoma cells exhibit increased ROS detoxification capacity
- PGC1α negative melanoma cells are more glycolytic and sensitive to ROS-inducing drugs

SIGNIFICANCE

Tumor cells reprogram a variety of central metabolic and bioenergetic pathways to maintain exacerbated growth and survival rates. The identification of the genetic factors responsible for specific metabolic programs is key to exploit this reprogramming for cancer therapy. Here, we show that in melanomas, overexpression of the transcriptional coactivator PGC1α, a key regulator of mitochondrial respiration, metabolically define melanoma tumors with high bioenergetic and ROS detoxification capacities. These metabolic capacities allow PGC1α positive melanomas higher rates of survival under oxidative stress compared to PGC1α negative melanomas. Our results underscore how different metabolic vulnerabilities defined by PGC1α expression could be therapeutically exploited to treat melanoma tumors.

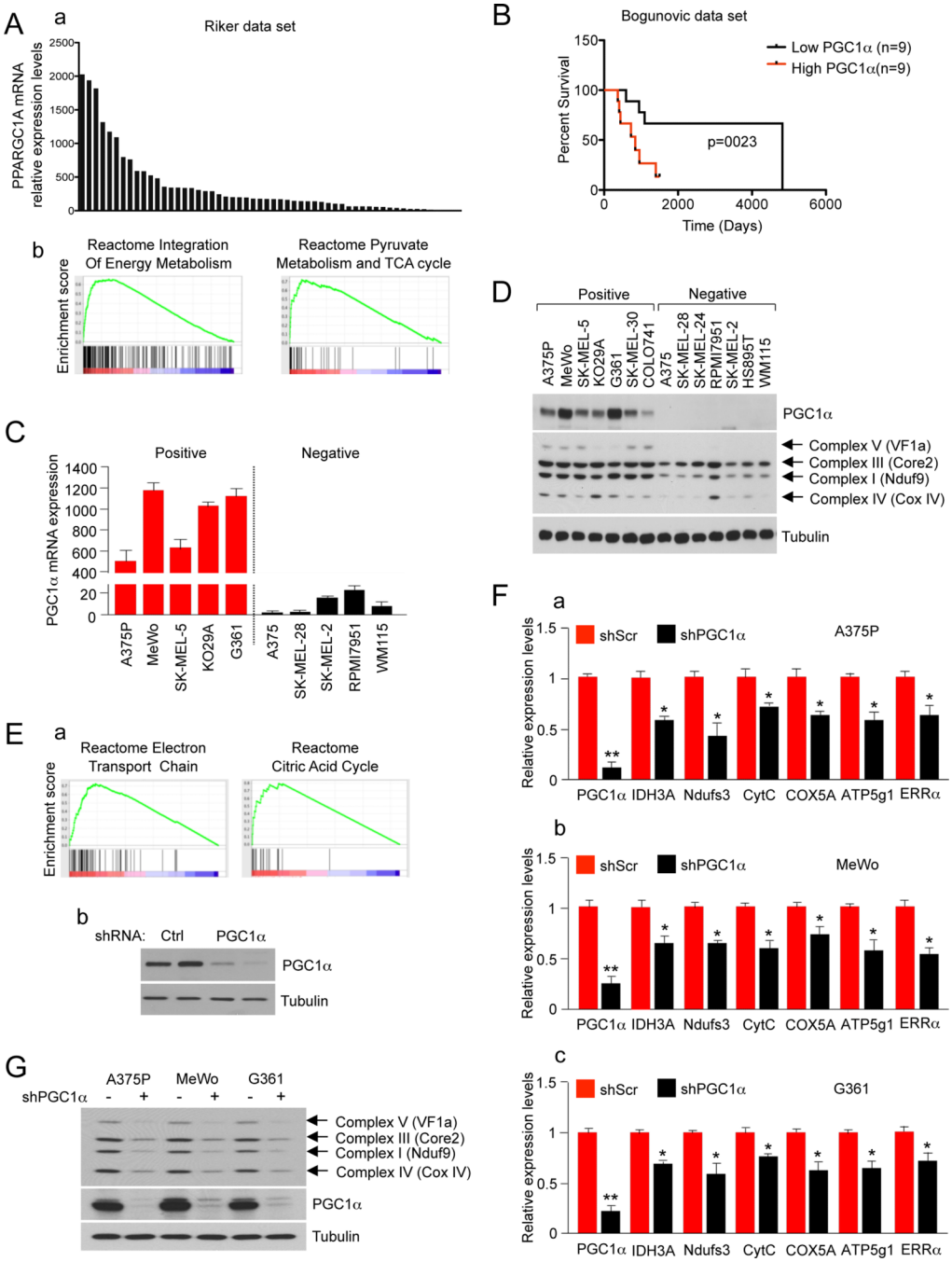

Figure 1. PGC1α Drives the Expression of a Mitochondrial Respiration Program in a Subset of Human Melanoma Tumors and Derived Cell Lines

(A) (a) Relative expression levels of PGC1α in 56 melanoma tumors included in the data set GSEA7553 (Riker et al., 2008). (b) Plots for two of the top gene sets from GSEA analysis of genes positively correlated with PGC1α expression.

(B) Kaplan-Meier survival curves for metastatic melanoma tumors with high and low PGC1α expression from dataset GSE19232 (Bogunovic et al., 2009). Survival curves for the 18 metastatic melanoma patients with tumors expressing the 25% highest and lowest PGC1α levels were calculated using Kaplan–Meier analysis with test of statistical significance using the Mantel–Cox log-rank test. The long-rank p value was 0.0230.

(C) PGC1α mRNA expression levels in 10 human melanoma cell lines. mRNA levels were quantified using qRT-PCR. Values represent mean ± SD of two independent experiments performed in triplicate.
(D) Protein levels of PGC1α and mitochondrial respiration-associated proteins in human melanoma cell lines.
(E) (a) Plots for two of the top gene sets of the GSEA analysis in control versus PGC1α knocked-down A375P cells. (b) PGC1α protein levels in the control and PGC1α knocked-down cells.
(F) mRNA levels of PGC1α mitochondrial target genes measured using qRT-PCR analysis after PGC1α knock-down in PGC1α positive cell lines: (a) A375P, (b) MeWo and (c) G361. Values represent mean ± SD of three independent experiments performed in triplicate. *$p < 0.05$ and **$p < 0.01$.
(G) Protein expression levels of mitochondrial respiration-associated proteins and PGC1α in A375P stably expressing a control or PGC1α shRNA.
See also Figure S1.

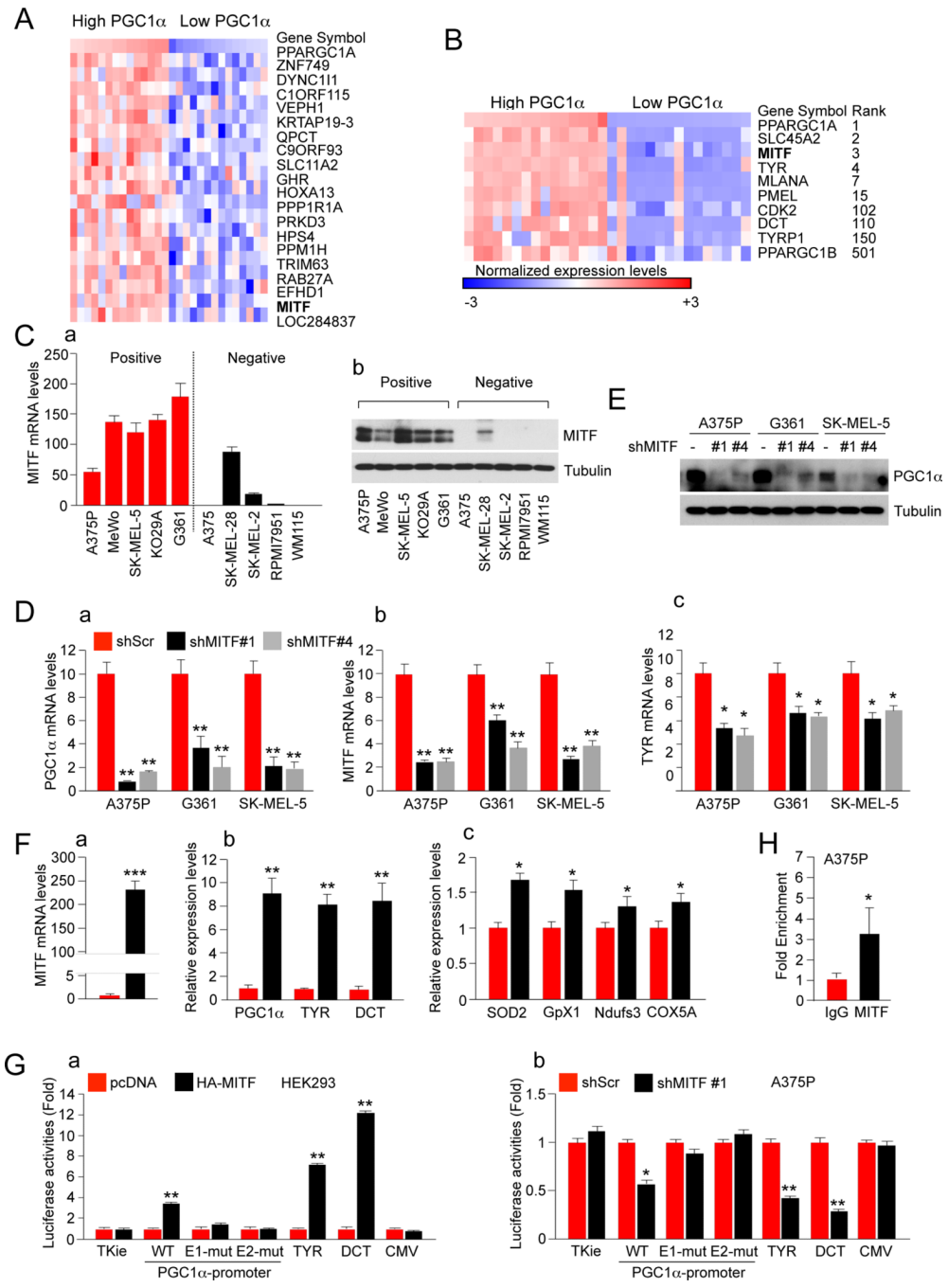

Figure 2. MITF is Necessary to Maintain High Levels of PGC1α Gene Expression in Melanoma Cells

(A) Heat map of the top 20 genes differentially expressed between the top and the bottom 25% melanoma samples ranked by PGC1α expression levels. Expression data was extracted from the GSE7553 data set. The gene list shown is ranked by signal to noise.

(B) Heat map of selected differentially expressed between the top and the bottom 25% melanoma samples ranked by PGC1α expression levels. Expression data was extracted from the CCLE database. The rank of the genes by signal to noise is shown.

(C) (a) MITF mRNA and (b) protein expression levels in 5 PGC1α positive and 5 PGC1α negative melanoma cell lines. Values represent mean ± SD of three independent experiments performed in triplicate.
(D) qPCR analysis of (a) PGC1α, (b) MITF targets and (c) TYR in shRNA MITF melanoma cell lines. Values represent mean ± SD of three independent experiments performed in triplicate. *$p < 0.05$ and **$p < 0.01$.
(E) Western blot analysis of PGC1α protein expression levels in shRNA MITF melanoma cell lines.
(F) qPCR analysis of (a) MITF, (b) MITF targets and (c) PGC1α target mRNAs in A375 melanoma cells ectopically expressing MITF. Values represent mean ± SD of two independent experiments performed in triplicate. *$p < 0.05$, **$p < 0.01$ and ***$p < 0.001$.
(G) PGC1α promoter luciferase analysis using transient transfection with the indicated plasmids performed in (a) 293 and (b) A375P cells. Values represent mean ± SD of two independent experiments performed in triplicate. *$p < 0.05$ and **$p < 0.01$. A representation of the construct is shown in figure S2D.
(H) ChiP analysis at the PGC1α promoter in A375P cells using an antibody against MITF and IgG as a control. Values represent mean ± SD of two independent experiments performed in triplicate. *$p < 0.05$.
See also Figure S2.

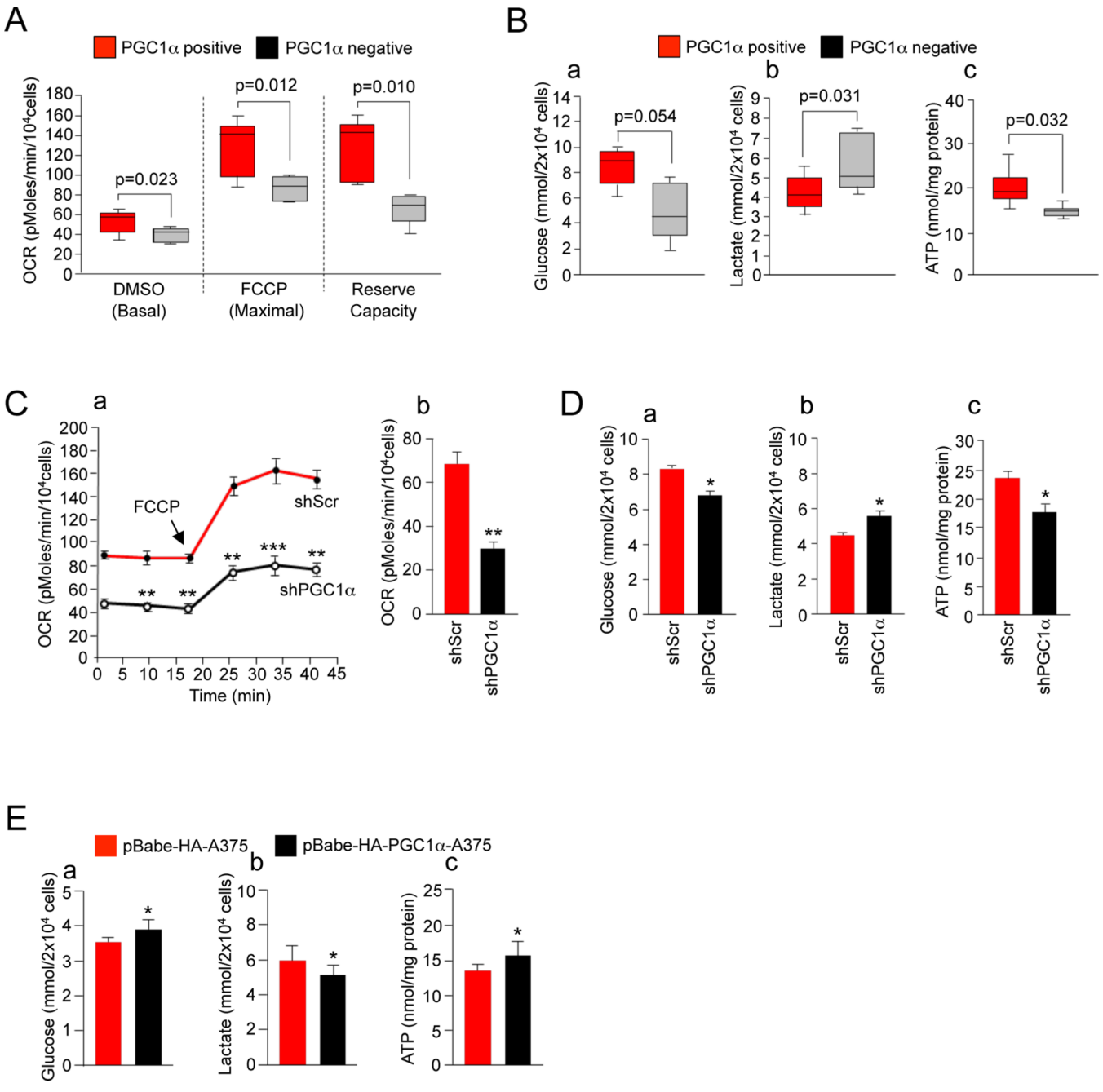

Figure 3. PGC1α Defines the Metabolic and Energetic Program of Human Melanoma Cells

(A) Basal and maximal oxygen consumption rates (OCR) in PGC1α positive and negative cells measured in DMSO control or FCCP treated cells. The reserve capacity was calculated by subtracting the basal from the maximum OCR. Values of two independent experiments performed in quadruplicate were averaged. The whiskers in the box plots represent the maximum and the minimum value.

(B) (a) Glucose (in the culture media), (b) lactate (in the culture media) and (c) intracellular ATP levels of PGC1α positive compared to PGC1α negative cells. Values of three independent experiments performed in duplicate were averaged. The whiskers in the box plots represent the maximum and the minimum value.

(C) (a) Real-time measurement of basal and maximal (after addition of FCCP) OCR and (b) basal OCR in control and PGC1α knock-down cells. Values represent mean ± SD of two independent experiments performed in quadruplicate. **$p < 0.01$.
(D) (a) Glucose (in the culture media), (b) lactate (in the culture media) and (c) intracellular ATP levels in control and PGC1α knock-down cells. Values represent mean ± SD of three independent experiments performed in duplicate. *$p < 0.05$.
(E) (a) Glucose (in the culture media), (b) lactate (in the culture media) and (c) intracellular ATP levels in cells overexpressing PGC1α. A375 cells stably expressing HA-PGC1α were used. Values represent mean ± SD of three independent experiments performed in duplicate. *$p < 0.05$.
See also Figure S3.

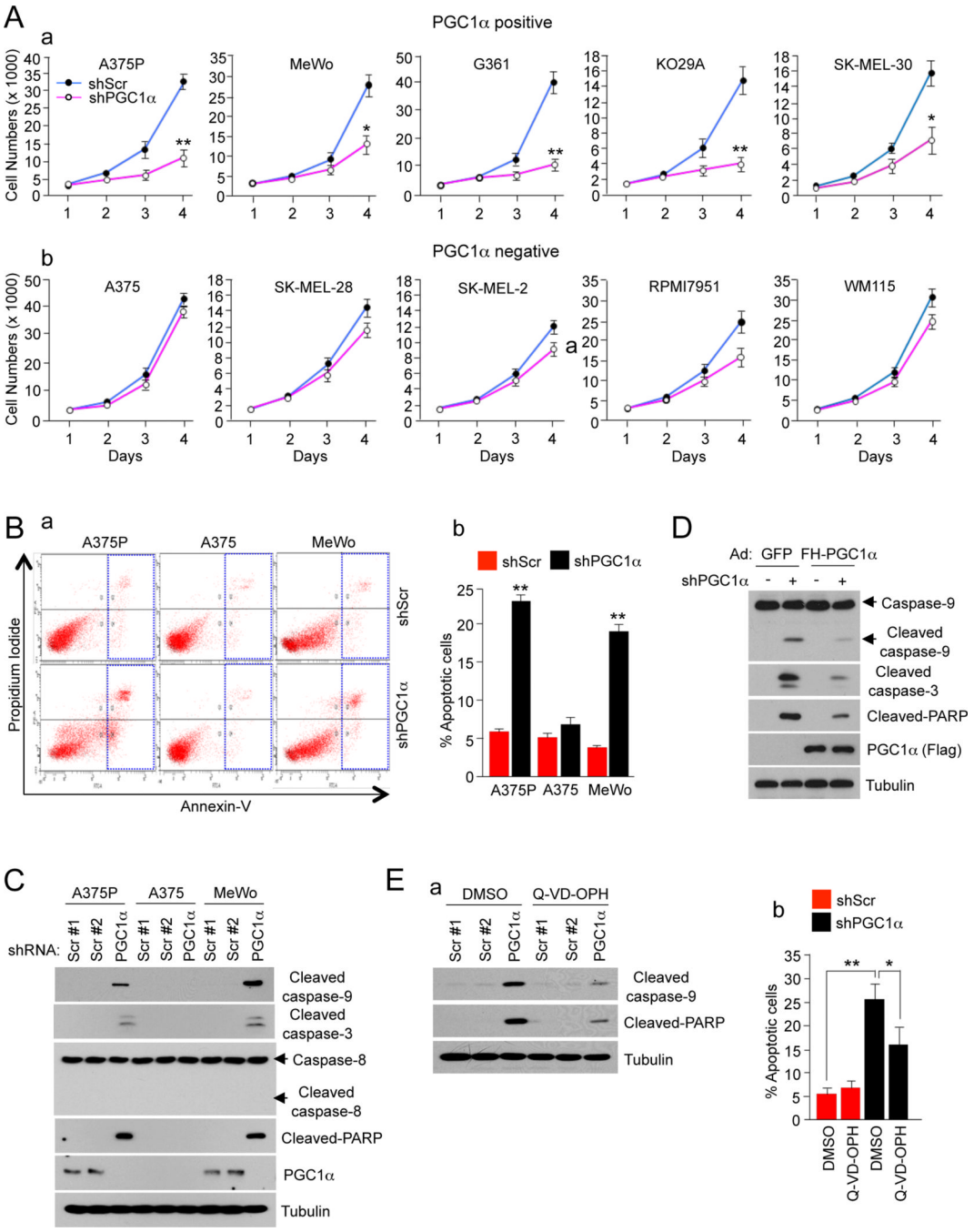

Figure 4. PGC1α is Essential for Survival and Tumor Progression

(A) Cell number analysis in PGC1α knock-down of (a) PGC1α positive and (b) PGC1α negative melanoma cells measured for 4 days after puromycin selection. Values on the graph represent mean ± SD of three independent experiments performed in quadruplicate. *p < 0.05 and **p < 0.01.

(B) (a) Annexin V analysis of apoptosis after PGC1α knock-down in PGC1α positive melanoma cells. (b) Quantitation of the percentage of apoptotic cells. Data represent mean ± SD of three independent experiments performed in triplicate. **p < 0.01.

(C) Western blot analysis of cleaved apoptotic proteins in PGC1α knocked-down and control melanoma cells.

(D) Western blot analysis of cleaved apoptotic proteins in ectopically expressed PGC1α in PGC1α knock-down A375P cells.
(E) Apoptosis measured by (a) western blot analysis of caspases and PARP cleavages or (b) Annexin V assays in PGC1α knocked-down and control A375P cells treated with 20 μM Q-VD-OPH (a pan-caspase inhibitor) for 2 days. Values on the graph represent mean ± SD of three independent experiments performed in triplicate. *$p < 0.05$ and **$p < 0.01$.
See also Figure S4.

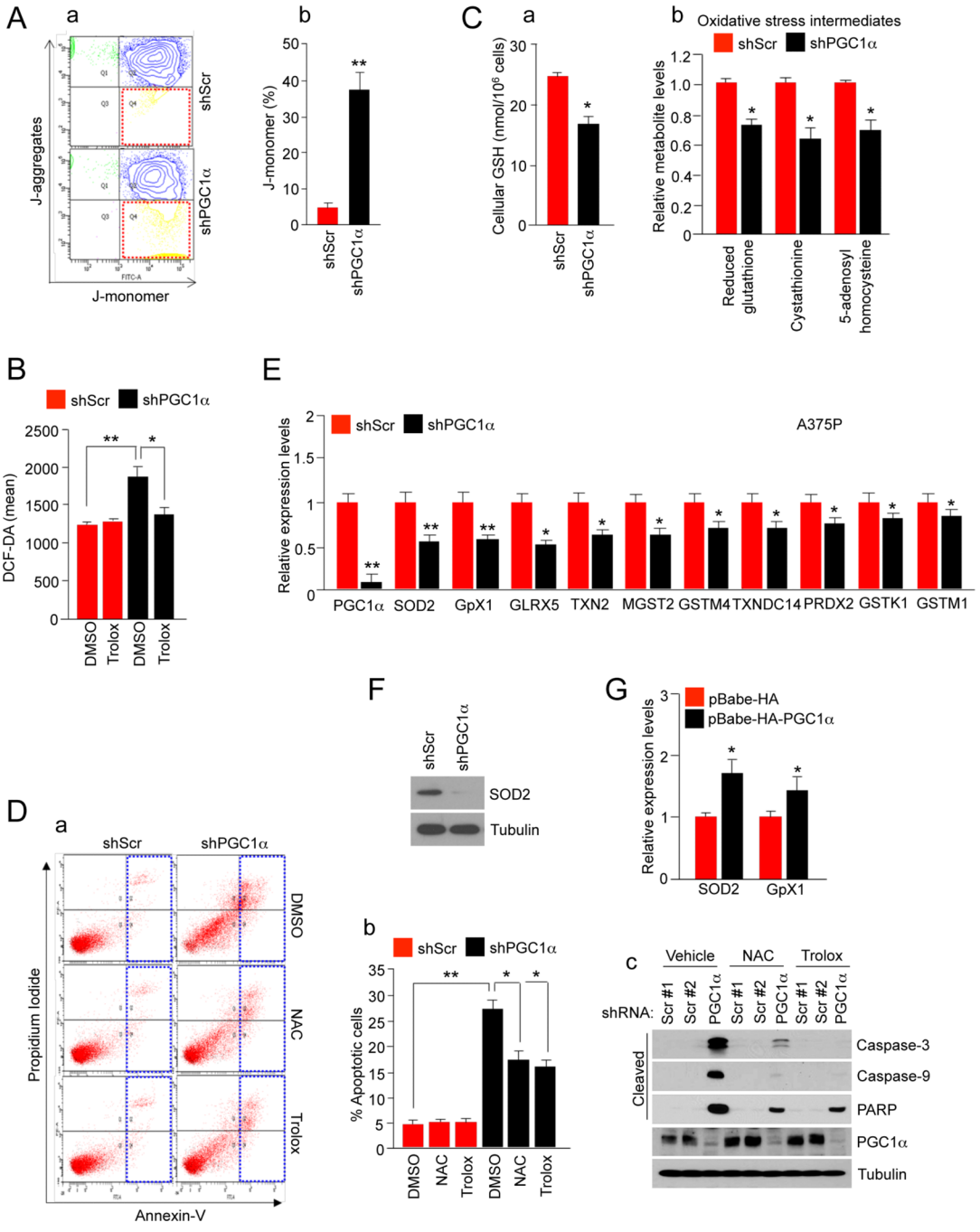

Figure 5. Depletion of PGC1α Triggers an Increase in ROS Levels Causing Apoptosis

(A) (a) Mitochondrial membrane potential measured by the JC-1 dye in PGC1α knocked-down and control A375P cells. (b) Quantitation of the percentage of J-monomer. Values on the graph represent mean ± SD of three independent experiments performed in duplicate. **p < 0.01.

(B) ROS levels in control and PGC1α knock-down A375P cells measured using the DCF-DA dye. Values represent mean ± SD of three independent experiments performed in triplicate. *p < 0.05 and **p < 0.01.

(C) (a) Total GSH levels and (b) oxidative stress intermediates in PGC1α knocked-down and control A375P cells. Values represent mean ± SD of three independent experiments performed in triplicate. *$p < 0.05$.
(D) Analysis of apoptosis in A375P cells (control and PGC1α knocked-down) treated with 2 mM NAC or 100 μM Trolox for 2 days. (a) Annexin V diagram, (b) quantitation of the percentage of apoptotic cells using the Annexin V assay and (c) western blot analysis of caspases and PARP cleavages. Values on the graph represent mean ± SD three independent experiments performed in triplicate. *$p < 0.05$ and **$p < 0.01$.
(E) mRNA expression levels of ROS detoxification genes in PGC1α knock-down A375P melanoma cells. Values represent mean ± SD of three independent experiments performed in triplicate. *$p < 0.05$ and **$p < 0.01$.
(F) Western blot analysis of SOD2 protein levels in A375P cells.
(G) SOD2 and GpX1 mRNA levels after ectopic expression of PGC1α in A375 cells. Values represent mean ± SD of two independent experiments performed in triplicate. *$p < 0.05$.
See also Figure S5.

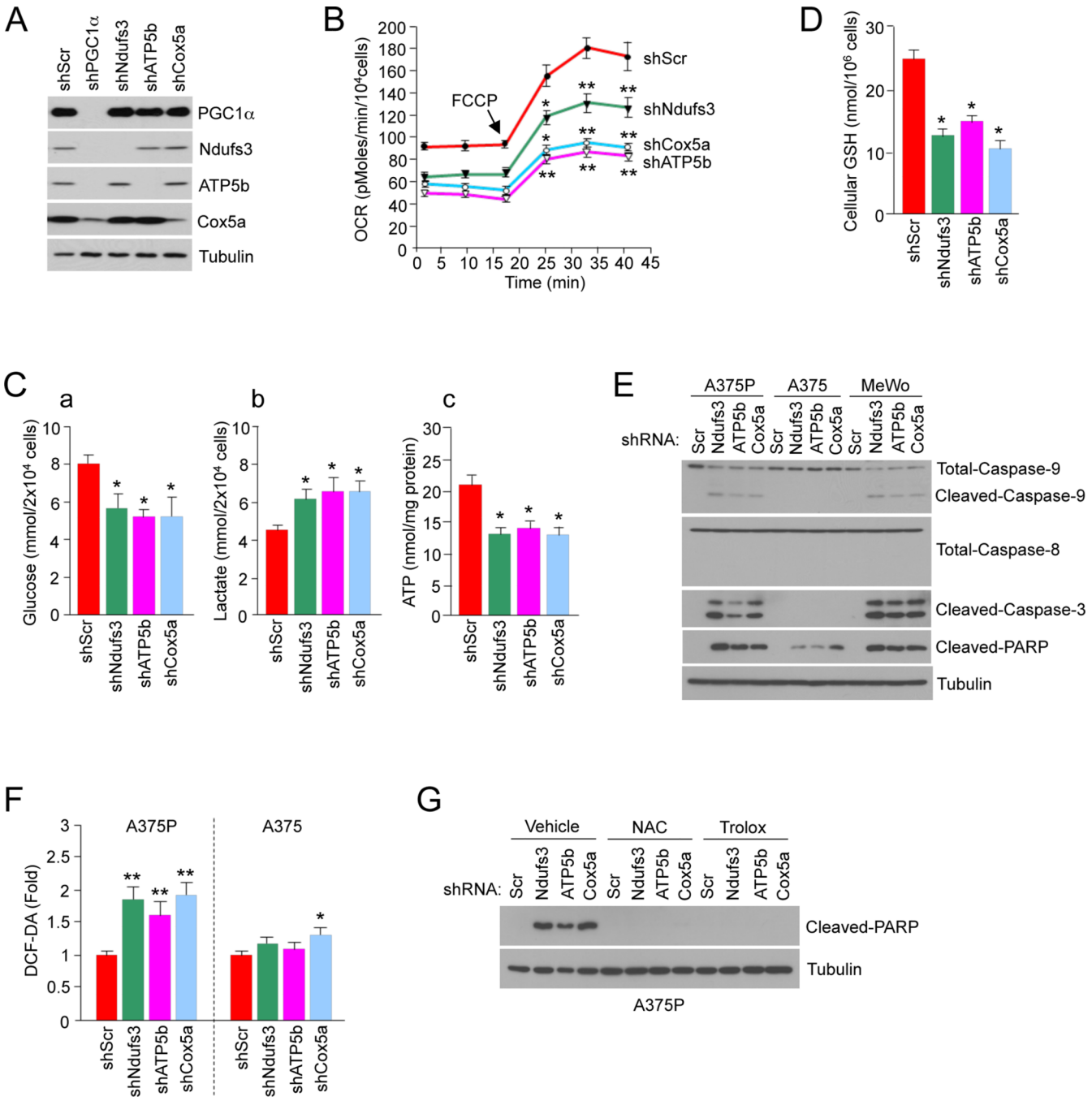

Figure 6. Induction of ROS-Mediated Apoptosis by Depletion of Mitochondrial Respiration PGC1α Target Genes

(A) Depletion of PGC1α and mitochondrial proteins in A375P melanoma cells.

(B) Real-time measurement of basal and maximal (after addition of FCCP) OCR after knock-down of the indicated genes encoding mitochondrial proteins in A375P. Values represent mean ± SD of two independent experiments performed in triplicate. *$p < 0.05$ and **$p < 0.01$.

(C) (a) Glucose (in the culture media), (b) lactate (in the culture media) and (c) intracellular ATP levels in A375P after knock-down of the indicated mitochondrial genes. Values represent mean ± SD of three independent experiments in duplicate. *$p < 0.05$.

(D) Cellular GSH levels in A375P after knock-down of the indicated mitochondrial genes. Values represent mean ± SD of three independent experiments in duplicate. *$p < 0.05$.
(E) Western blot analysis of apoptotic markers after knock-down of the indicates genes mitochondrial proteins in PGC1α positive cells.
(F) ROS levels, measured by DCF-DA fluorescent dye, after depletion of mitochondrial proteins in A375P or A375 cells. Values represent mean ± SD of three independent experiments in duplicate. *$p < 0.05$ and **$p < 0.01$.
(G) Protein expression levels of cleaved-PARP after depletion of mitochondrial proteins in A375P cells treated with the indicated antioxidants.

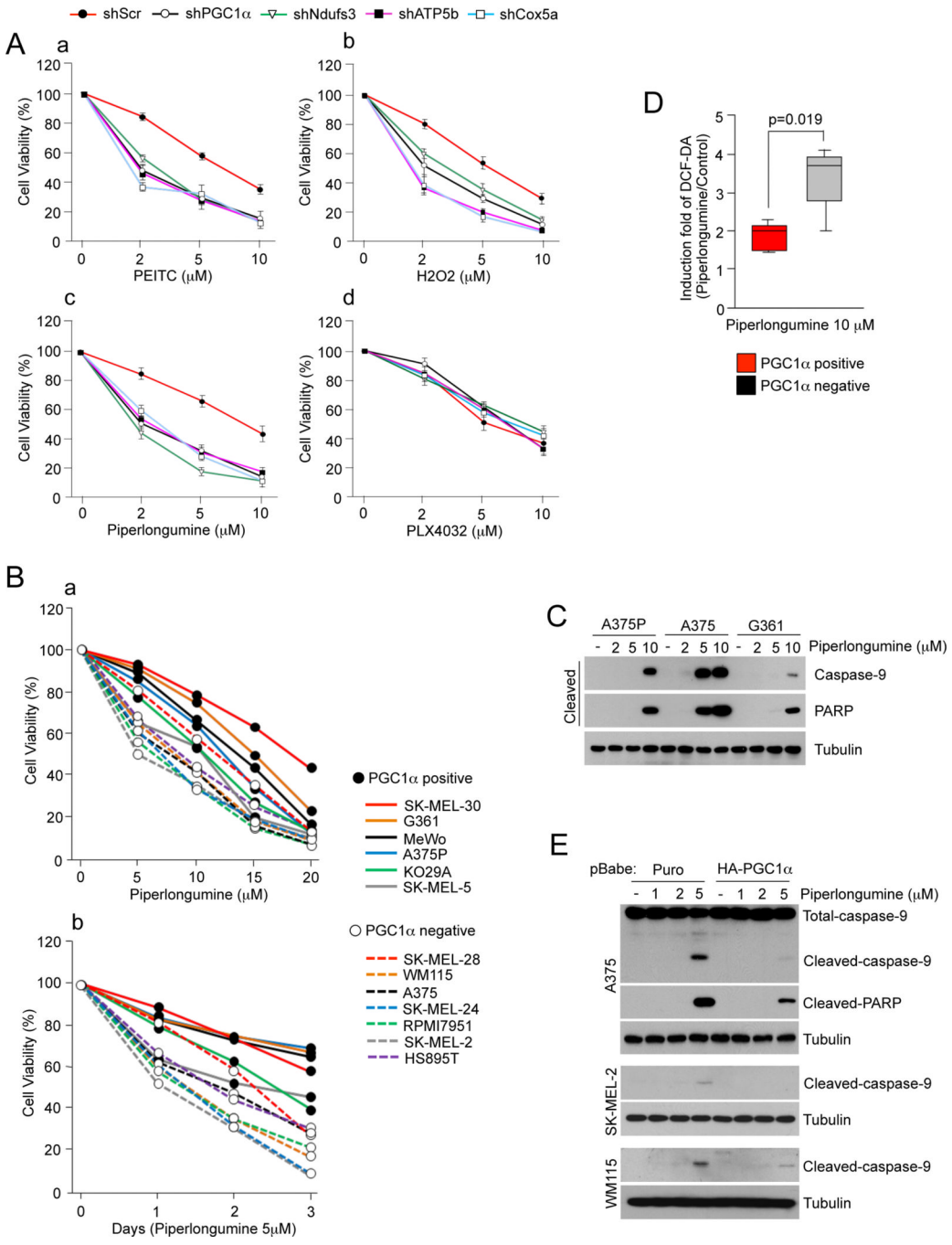

Figure 7. PGC1α Expression Decreases Apoptotic Sensitivity to ROS-Inducing Drugs in Human Melanoma Cells

(A) Cell viability, measured using cell titer glo, after treatment with (a) PEITC, (b) H2O2, (c) piperlongumine and (d) PLX4032 in A375P cells stably expressing the indicated shRNAs. Values represent mean ± SD of three independent experiments in triplicate.

(B) Cell viability of PGC1α positive and negative melanoma cell lines treated with piperlongumine at (a) different concentrations and (b) times. Values represent mean of three independent experiments in triplicate.

(C) Analysis of cleaved Caspase-9 and PARP in two PGC1α positive (A375P and G361) and one PGC1α negative (A375) cell lines treated with piperlongumine.

(D) ROS levels in PGC1α positive melanoma cell lines treated with piperlongumine. Values of three independent experiments performed in duplicate were averaged. The whiskers in the box plots represent the maximum and the minimum value.
(E) Analysis of apoptosis using cleavage of apoptotic markers in PGC1α negative melanoma cell lines ectopically expressing PGC1α and treated with piperlongumine.
See also Figure S7.

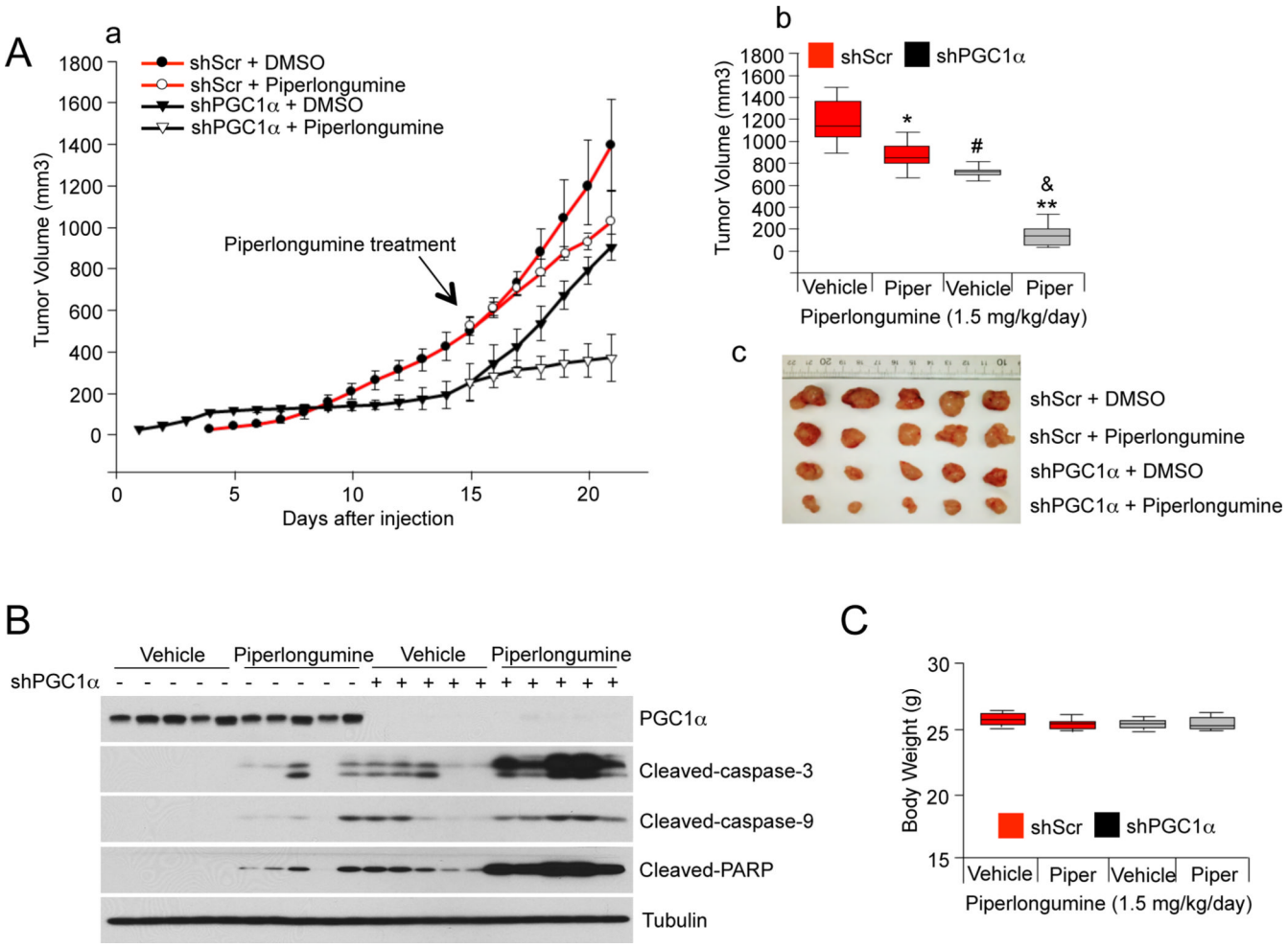

Figure 8. PGC1α Expression Decreases Apoptotic Sensitivity to ROS-Inducing Drugs in Human Melanomas

(A) (a) Tumor volume analysis of xenografts of A375P cells expressing shRNAs against PGC1α or control shRNAs. 15 days after cell injection, mice were injected daily with piperlongumine (1.5 mg/kg) or DMSO. The tumor growth curves are plotted as mean ± SEM (n = 10, each group). Statistical significance of tumor volumes were calculated by one-way ANOVA with a Tukey post test; *$p < 0.05$; **$p < 0.01$, DMSO vs piperlongumine; $^{\#}p < 0.05$, DMSO/control shRNA vs DMSO/PGC1α shRNA; $^{\&}p < 0.01$, piperlongumine/control shRNA vs piperlongumine/PGC1α shRNA. (b) In the box plots, final tumor volumes are represented (n=10). The whiskers in the box plots represent the maximum and the minimum value. (c) Representative images of tumors are shown.

(B) Western blot analysis of apoptotic cleaved caspases and PARP in PGC1α knocked-down tumors treated with piperlongumine.

(C) Body weight measured at the end of experiment. The whiskers in the box plots represent the maximum and the minimum value.

Table 1

GSEA analysis of genes ranked by positive correlation with PGC1α expression in melanoma tumors. Gene expression of 56 melanoma tumors extracted from the GSEA7553 data set (Riker et al., 2008) was ranked for positive correlation with PGC1α expression and analyzed with the GSEA algorithm using the reactome gene sets, the significant (q<0.25) gene sets ranked by normalized enrichment score are shown.

NAME	NES	FDR q-val
REACTOME_INTEGRATION_OF_ENERGY_METABOLISM	2.15	0.02
REACTOME_GLUCOSE_REGULATION_OF_INSULIN_SECRETION	2.08	0.03
REACTOME_REGULATION_OF_INSULIN_SECRETION	2.09	0.04
REACTOME_PYRUVATE_METABOLISM_AND_TCA_CYCLE	1.94	0.1
REACTOME_CITRIC_ACID_CYCLE	1.88	0.13
REACTOME_PEROXISOMAL_LIPID_METABOLISM	1.88	0.16
REACTOME_ELECTRON_TRANSPORT_CHAIN	1.86	0.13